Absorption edge of the amorphous $(GeS_2)_x(As_2S_3)_{1-x}$ system under hydrostatic pressure

Seinosuke Onari, Takao Inokuma, Hiromichi Kataura, and Toshihiro Arai
Institute of Applied Physics, University of Tsukuba, Sakura, Ibaraki 305, Japan
(Received 24 July 1986)

The transmission spectra of the amorphous semiconductor system $(GeS_2)_x(As_2S_3)_{1-x}$ are measured under hydrostatic pressure, and the dependence of the optical gap E_0 and the refractive index n on the pressure is studied. The large red shift in E_0 is attributed to the band-broadening effect originating in the increased interaction between the lone-pair electrons of the sulfur atoms. The change in the refractive index n is analyzed successfully by the Penn-Phillips-type two-oscillator model. Anomalous changes in the optical gap E_0 are observed for GeS_2-rich materials in the pressure range $20 \lesssim P \lesssim 40$ kbar. Corresponding to these anomalies, a large hysteresis is also observed in the experimental curve of the optical gap E_0 versus pressure P. This anomaly is attributed to a structural change induced by pressure, and this suggests the existence of voids in the GeS_2-rich amorphous $(GeS_2)_x(As_2S_3)_{1-x}$ system.

I. INTRODUCTION

The effect of compression on the optical dielectric constant of solids has attracted much interest and it has been treated by many authors.[1] Van Vechten[2] showed that a Penn-Phillips-type single-oscillator model could successfully treat covalent and ionic crystals. In particular this model could explain the qualitatively different behavior of the Grüneisen parameter defined by $\chi' = -d\ln\chi/d\ln V$ for the covalent Ge family ($\chi' < 0$) and for alkali halides ($\chi' > 0$), where $\chi = (\epsilon_0 - 1)/4\pi$ is the electronic susceptibility.

The effect of compression on the optical dielectric constant for chalcogenide amorphous materials has been shown to be large and characteristic.[3-9] Namely, the band-gap energy shows a strong red shift to low energy with increasing pressure, while the refractive index n shows a rapid increase with increasing pressure. Weinstein *et al.* have studied the optical-gap behavior of a-As_2S_3 (Refs. 4 and 5) and a-GeS_2 (Ref. 6) under hydrostatic pressure and interpreted the experimental results in terms of the network dimensionality of these molecular solids.

In the present paper, the effect of hydrostatic pressure on the optical gap is studied in detail on the $(GeS_2)_x(As_2S_3)_{1-x}$ system for the first time. An anomalous dependence of the optical gap on the pressure and large hysteresis effects for GeS_2-rich amorphous materials are observed. These anomalies are attributed to the structural change produced by the pressure, and the possibility is discussed of the existence of a hollow structure, like that seen in a three-dimensional GeS_2 crystal.[10] The effect of compression on the optical dielectric constant of the $(GeS_2)_x(As_2S_3)_{1-x}$ system is analyzed successfully by the Penn-Phillips-type two-oscillator model.

II. EXPERIMENTAL PROCEDURE

The samples used were prepared by the melt quenching of a mixture of elements Ge, As, and S of high purity (99.9999%-purity stock) for the composition $(GeS_2)_x(As_2S_3)_{1-x}$; $x = 0.0$, 0.25, 0.50, 0.75, 0.90, and 1.0. The sample materials were sealed at 10^{-6} Torr in a quartz ampoule, and heated gradually up to 800 °C and the furnace was rocked for 12 h in order to obtain homogeneous samples. For all compositions except $x = 0.0$ and 1.0, samples were rocked for 72 h at 950—1000 °C, and then were quenched in air. The sample for $x = 0.0$ was rocked for 24 h at 600 °C and then was quenched in air. For the composition $x = 1.0$, the ampoule was water quenched in order to prevent crystallization.

The glass transition temperature of the $(GeS_2)_x(As_2S_3)_{1-x}$ system was measured in the temperature range of 300—700 K by differential scanning calorimetry (DSC) measurement (Seikosha Model No. SSC-560S). The rate of temperature rise was 10 °C/min. DSC measurements confirmed that the sample was one phase and that crystals are not included.

The composition ratios of the samples were examined by a Jarrel-Ash inductivity coupled argon plasma (optical emission spectroscopy, Model 975, Plasma Atom Comp.), and the maximum compositional deviation in weight from the intended composition was found to be less than ±1%.

The samples were sliced and polished to a thickness of 10—20 μm. The thicknesses of the samples were 13.8, 19.4, 13.5, 14.1, 15.5, and 20.0 μm for the compositions $x = 0.0$, 0.25, 0.50, 0.75, 0.90, and 1.0, respectively. These small pieces were installed in a diamond anvil cell. The pressure was monitored by the wavelength of the R_1 luminescence line from a small piece of ruby installed in the diamond anvil cell. As a pressure-transmitting medium a mixture of a methanol and ethanol in the ratio of 4:1 was used. The pressure was monitored before and after the transmission measurement and the error of the pressure measurement was determined by the uncertainty of the ruby scale, i.e., about ±3%.

Transmission measurements were performed with the monochromater JASCO-CT-25C. Light passing through the sample was focused by a lens onto a small hole in a

screen in the image plane and the transmission measurement was performed. The sample was set behind the monochromator. The monochromatic light incident on the sample was too weak to induce the photostructural change. As a light source, a halogen lamp and a xenon lamp were used. In the wavelength range longer than 8000 Å, a PbS detector was used. A photomultiplier R-374 was used in the wavelength range shorter than 8000 Å. The pressure dependence of the refractive index n was obtained from the interference fringe spacing in the transparent region.

III. RESULTS

A. Transmission spectra and the absorption edge

The absorption spectra of the $(GeS_2)_x(As_2S_3)_{1-x}$ system for various composition x at the atmospheric pressure are shown in Fig. 1. The energy range of these spectra corresponds to that of the Urbach tail. The exponential slope of the absorption coefficient is shown to depend on the composition x.

The transmission spectra at various pressures are shown in Fig. 2. The total fraction of light transmitted is corrected for reflection and other losses and standardized relative to the (constant) transmission at longer wavelengths. For every composition x, the transmission spectra are shifted to the low-energy side with increasing pressure and the spectra obtained were nearly parallel to each other. When the pressure is removed, the absorption edge shifts back to the high-energy side, but with hysteresis. After the pressure is removed, the absorption edge initially remains at a lower energy than the original value, but slowly increases. The dependence of the optical gap E_0 on the pressure is shown in Fig. 3.

When the interference effects are ignored, the transmission T is expressed as follows:

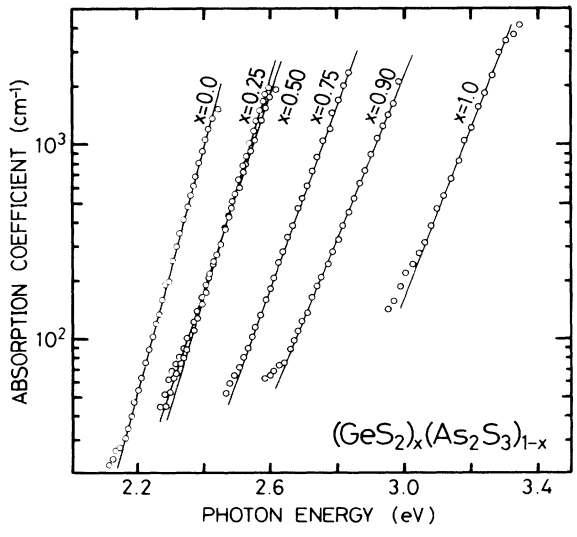

FIG. 1. Absorption coefficient of $(GeS_2)_x(As_2S_3)_{1-x}$ at room temperature for $x=0.0$, 0.25, 0.50, 0.75, 0.90, and 1.0.

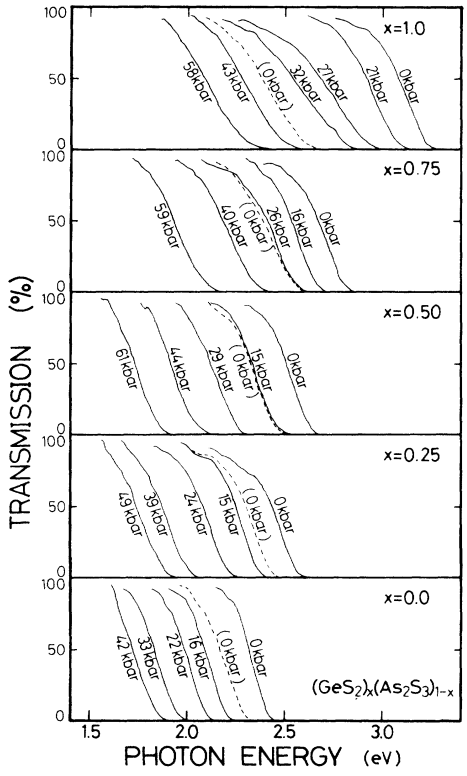

FIG. 2. Transmission spectra of $(GeS_2)_x(As_2S_3)_{1-x}$ under hydrostatic pressure. Dotted curves are the transmission spectra after the pressure is released.

$$T=\frac{(1-R)^2e^{-\alpha l}}{1-R^2e^{-2\alpha l}}\ , \tag{1}$$

where R is the reflectivity, α is the absorption coefficient, and l is the thickness of sample. Under the condition $R^2e^{-2\alpha l}\ll 1$, T is expressed by the relation

$$T=(1-R)^2e^{-\alpha l}\ . \tag{2}$$

Furthermore, when the transmission is normalized by the constant transmission $T'=(1-R)^2$ in the transparent region as in the present case, T is expressed simply by

$$T=e^{-\alpha l}\ . \tag{3}$$

In our present experiment, the optical gap E_0 is defined as the energy at $\alpha=5\times10^2\ \mathrm{cm}^{-1}$. The thickness of the sample was measured by the interference pattern in the transmission spectra by the relation as follows:

$$l=\frac{1}{2n}\left[\frac{1}{\lambda_{m+1}}-\frac{1}{\lambda_m}\right]^{-1}\ , \tag{4}$$

where λ_m is the peak wavelength in the interference pattern. The refractive index n is obtained from the measurement of the Brewster angle.

In Fig. 3, the optical gap E_0 for the first compression is shown by the solid circles and the optical gap E_0 for the second compression some days after the first compression is shown by the open circles. E_0 shows a red shift with

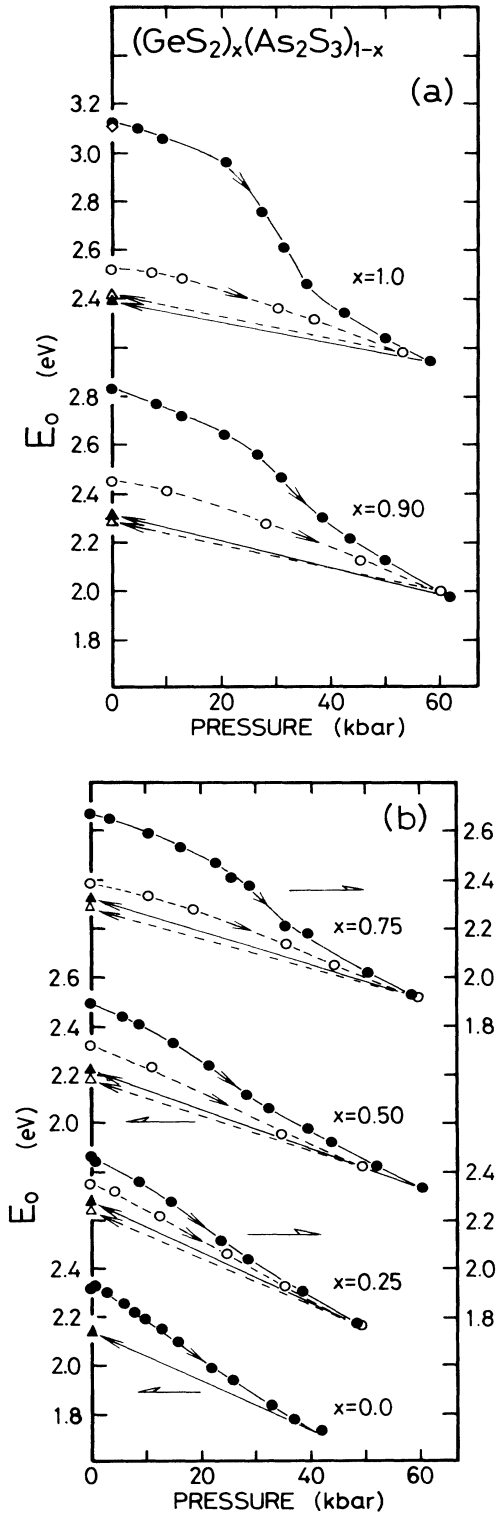

FIG. 3. Dependence of the optical gap E_0 upon the applied hydrostatic pressure. Solid circles represent the first compression, solid triangles represent the optical gap just after the release of the pressure, open circles represent the second compression, and open triangles represent the optical gap just after the release of the second compression. The square mark denotes the optical gap after annealing.

increasing pressure for every composition x. Furthermore, for the samples $x \geq 0.5$, the pressure coefficient dE_0/dP changes drastically at a particular pressure. The optical gap E_0 after the release of the second compression is also shown in Fig. 3. An anomalous change in the optical gap E_0 with pressure is observed only for the virgin sample. The optical gaps E_0 at the highest pressure of approximately 60 kbar become approximately the same for the first and second compression. Large hysteresis is seen only after the first compression.

B. Refractive index n

Dependence of the optical path length nl on the hydrostatic pressure is shown in Fig. 4. In these figures, optical path length nl is shown normalized relative to the value at the atmospheric pressure. For each composition x, the optical path length nl is observed to increase with increasing pressure. The observed trend is that the pressure coefficient of nl decreases with increasing composition x of the GeS_2. For $x = 1.0$, GeS_2, the interference pattern could not be observed because of the low reflectivity, and the value from Ref. 6 has been used in the discussion.

C. Glass transition temperature

In Fig. 5, the glass transition temperature T_g derived from the DSC measurement is shown. For GeS_2, T_g is out of the range of our DSC equipment and the value of T_g from Ref. 11 is employed in the discussion.

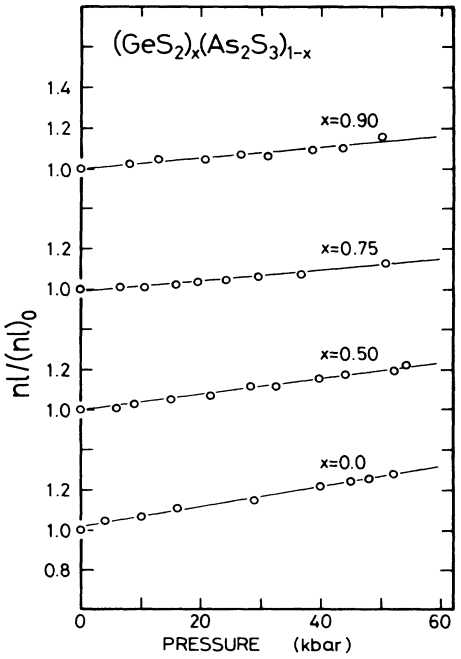

FIG. 4. Dependence of $nl/(nl)_0$ on the hydrostatic pressure for $(GeS_2)_x(As_2S_3)_{1-x}$.

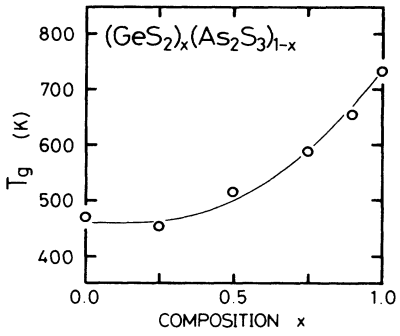

FIG. 5. Glass transition temperature T_g is plotted as a function of the composition x for $(GeS_2)_x(As_2S_3)_{1-x}$.

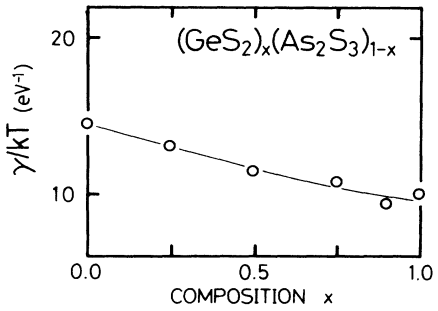

FIG. 7. γ/kT is plotted as a function of the composition x for $(GeS_2)_x(As_2S_3)_{1-x}$. The definition of γ is seen in the text.

IV. DISCUSSION

A. Dependence of the optical gap E_0 on the composition x

The dependence of the optical gap E_0 on the composition x at atmospheric pressure is shown in Fig. 6. The optical gap E_0 can be seen to increase gradually up to $x=0.5$. However, the optical gap E_0 increases steeply for $x \geq 0.5$ with increasing GeS_2 concentration. In the As_2S_3-rich region the optical gap E_0 is apparently determined by the energy gap of the As_2S_3 component. However, in the GeS_2-rich region, the optical gap E_0 becomes nearly that of GeS_2. The absorption in our measurement is in the range of the Urbach tail and the absorption coefficient α is expressed as follows:

$$\alpha(\omega) \propto \exp\left[\frac{\gamma(\hbar\omega - E_0)}{kT}\right], \tag{5}$$

where γ is a constant, T is a temperature, and k is the Boltzmann constant. γ/kT is plotted in Fig. 7 as a function of the composition x. $1/\gamma$ is a measure of the disorder of the system.[12] Decrease of γ/kT with the increase of the GeS_2 means that the exponential tail is extended deep into the band gap for GeS_2. In other words, the disorder of the system increases with the increasing GeS_2 concentration.

B. Dependence of the optical gap E_0 on the pressure

In the molecular-type amorphous materials, each molecular unit is bonded weakly by a van der Waals force originating in the lone-pair electron of a S atom.

In the system $(GeS_2)_x(As_2S_3)_{1-x}$ the top of the valence band is composed of the lone-pair electrons of sulfur atoms, and the bottom of the conduction band is composed of the antibonding states of Ge and As atoms.

The covalent bond is comparatively incompressible. However, the distances between the molecular units bonded by the van der Waals forces are more strongly compressed. As a result, the interaction among the lone-pair electrons is increased and band broadening is induced. This results in the red shift of the optical gap E_0 with increasing hydrostatic pressure. In Fig. 8, the schematic density-of-states diagram is shown. This kind of red shift is also observed in the low-dimensional crystals containing chalcogenide atoms.

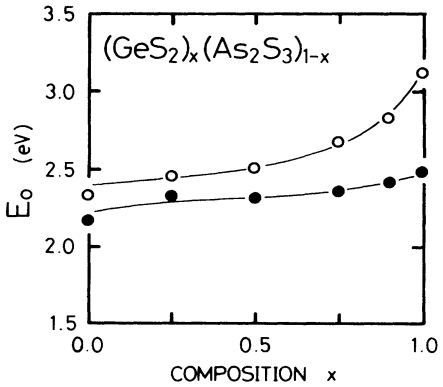

FIG. 6. Optical gap E_0 at $P=0$ kbar is plotted as function of the composition x for $(GeS_2)_x(As_2S_3)_{1-x}$.

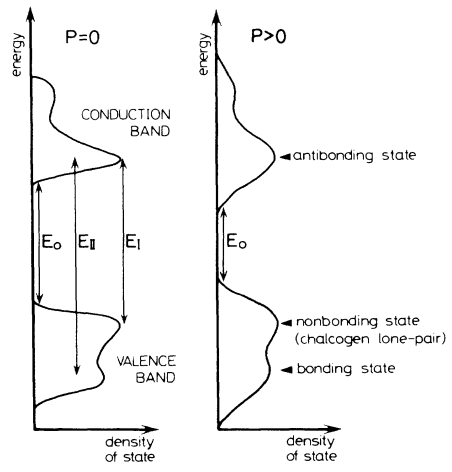

FIG. 8. Schematic diagram of the energy vs density of state for $P=0$ (left side) and $P>0$ (right side).

The pressure coefficient dE_0/dP at atmospheric pressure is obtained from a least-squares fit. In Fig. 9, the value of the pressure coefficient $-dE_0/dP$ is plotted as a function of the composition x. As the pressure dependence is nonlinear at a pressure higher than 20 kbar, the fitting was done here for a pressure lower than 20 kbar. $-dE_0/dP$ is seen to decrease almost linearly with the increase of the GeS_2 composition x. A sudden change of dE_0/dP was observed at $P \approx 20$ kbar for GeS_2-rich composition. At $x=0.5$, this sudden change in dE_0/dP began to appear, and as x increased the change became more pronounced. The value of the sudden change of $-dE_0/dP$ near $P \approx 20$ kbar, for example, is $1.19 \rightarrow 1.63$ for $x=0.5$, $0.90 \rightarrow 1.80$ for $x=0.75$, $0.92 \rightarrow 2.22$ for $x=0.90$, and $0.81 \rightarrow 3.55$ for $x=1.0$ (here the units of $-dE_0/dP$ are 10^{-2} eV/kbar). The appearance of this effect for $x \geq 0.5$ is correlated with the trend of the change of E_0 with the increase of the GeS_2 concentration x. In Ref. 6 no measurement was reported for the pressure between 0 and 26 kbar, and the reported value of $dE_0/dP=23$ meV/kbar for GeS_2 was obtained by connecting the E_0 at $P=0$ and $P=26$ kbar by the straight line. The value of dE_0/dP in Ref. 6 is, however, in good agreement with our experiment in the pressure range above 20 kbar.

GeS_2 has two types of crystal structure.[10] One is the two-dimensional GeS_2 which is usually obtained at a relatively high temperature, and the other is the three-dimensional GeS_2 crystal with the same local structure (i.e., nearest-neighbor bonding) as SiO_2, as shown in Figs. 10(a) and 10(b), respectively.

In the amorphous GeS_2, network structure may be composed of the mixture of the two types of crystal structures mentioned above. It may be of importance to notice the existence of voids in the three-dimensional GeS_2. It is possible that similar void structures may also exist in the amorphous GeS_2. In the high-pressure region of $P \geq 20$ kbar, the void may be crushed to some extent by the compression, and this induces a larger overlap between the S lone-pair electrons. This may be the origin of the large value of $-dE_0/dP$ observed in the pressure region $20 \leq P \leq 40$ kbar.

As shown in Fig. 3, hysteresis in E_0 is observed after the pressure is released. E_0' is defined as the optical gap at 24 h after the release of the pressure. E_0^{hyst} is defined as $E_0^{\text{hyst}}=E_0(P=0)-E_0'$. The value of E_0^{hyst} for each composition x is shown in Fig. 11. This shows that E_0^{hyst} is almost constant up to $x=0.5$, and it is increased with the increase of x for $x \geq 0.5$. E_0^{hyst} of GeS_2 (0.63 eV) is large compared with that of As_2S_3 (0.16 eV).

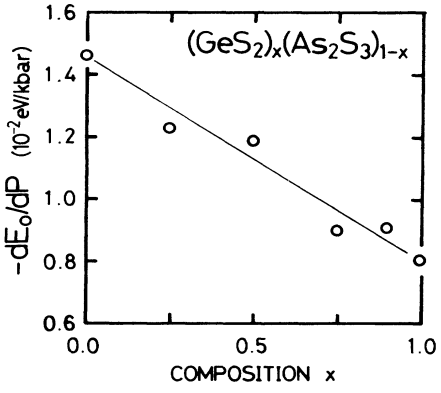

FIG. 9. $-dE_0/dP$ for the low-pressure region is plotted as a function of the composition x for $(GeS_2)_x(As_2S_3)_{1-x}$.

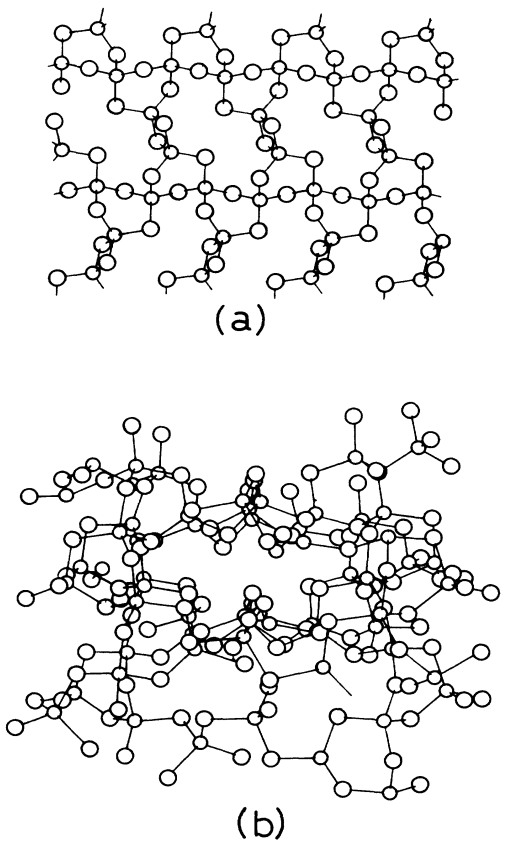

FIG. 10. (a) Crystal structure of the two-dimensional GeS_2. (b) Crystal structure of the three-dimensional GeS_2.

Now we will further discuss the relation between E_0^{hyst} and the nonlinear behavior of E_0 with changing pressure. As seen in Fig. 3, a large change in E_0 occurs in the pressure range $20 \lesssim P \lesssim 40$ kbar for $x \geq 0.5$. The change of E_0 with pressure is closely correlated with E_0^{hyst} for each composition. Namely, the larger the change of E_0 in the pressure range $20 \lesssim P \lesssim 40$ kbar, the larger is the value of E_0^{hyst}.

As seen in Fig. 3, the change of E_0 on the second compression shows no anomalous dependence on pressure, and the value of E_0 near the maximum pressure (50—60 kbar) is almost the same as that of the first compression. The behavior after the release of the first compression is almost uniform for the second compression. These experiments suggest that a structural change occurs in the pressure range near 20 kbar. This structural change still remains after the pressure is removed, and it appears as a pronounced hysteresis. It may be of interest to mention

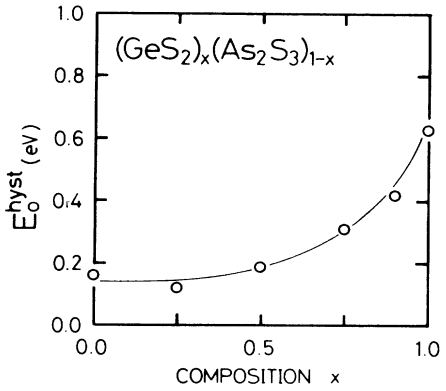

FIG. 11. E_0^{hyst} is plotted as a function of the composition x for $(GeS_2)_x(As_2S_3)_{1-x}$. See the definition of E_0^{hyst} in the text.

the phase transition of three-dimensional GeS_2 at 110 kbar.[6] In the case of this phase transition, the color changes from colorless to brown, and the absorption edge shifts discontinuously to the red by about 1 eV. Furthermore, the high-pressure phase remains after the pressure is removed. These effects have been interpreted as the destruction of the void structure characteristic of the three-dimensional GeS_2 crystal.

After the annealing of these amorphous materials at 400 °C for 2 h, the optical gap E_0 has a value very similar to that of the virgin sample before the compression. The structure under the high pressure is still in the metastable state, and the void structure may be recovered easily with annealing.

Comparing Figs. 5 and 11 we can also see that there is a strong correlation between E_0^{hyst} and the glass transition temperature T_g.

C. Dependence of the refractive index n on the pressure

In Fig. 4, the optical path length nl is plotted as a function of pressure, and the value of $(1/n)(dn/dP)$ can be obtained. n is the refractive index and l is the thickness of sample. From the relation

$$\frac{1}{n}\frac{dn}{dP}=\frac{1}{nl}\frac{d(nl)}{dP}+\frac{K}{3}\ , \tag{6}$$

$(1/n)(dn/dP)$ is calculated. Lame's constants are determined from the longitudinal and transverse sound velocities determined[13] by the pulse echo method, and the compressibility K is calculated from the Lame's constants. The values of $(1/n)(dn/dP)$ are 7.88 for $x=0.0$, 5.32 for $x=0.5$, 5.32 for $x=0.75$, and 5.36 for $x=0.9$, in units of 10^{-3} kbar^{-1}.

In the case of the $(GeS_2)_x(As_2S_3)_{1-x}$ system, the weak bond between the molecular units is shortened under compression, and the covalently bonded nearest-neighbor atoms may not be influenced as much. Therefore, bonding-antibonding interaction is not increased as much.

As seen in Fig. 8, the valence bands of these amorphous systems are composed of two bands. One is the nonbonding state of lone-pair electrons of chalcogen atoms, and the other is the low-lying bonding state. We consider the transition from the nonbonding state to the antibonding state (region I) and the transition from the bonding state to the antibonding state (region II). To discuss these two transitions, the Penn-Phillips-type two-oscillator model proposed by Weinstein *et al.*[5] is used.

The electronic susceptibility is then expressed as follows:

$$\chi=\chi_{\text{I}}+\chi_{\text{II}}=\frac{\hbar^2e^2}{m}\frac{n_{\text{I}}f_{\text{I}}}{VE_{\text{I}}^2}+\frac{\hbar^2e^2}{m}\frac{n_{\text{II}}f_{\text{II}}}{VE_{\text{II}}^2}\ . \tag{7}$$

Here the subscripts I and II refer to the regions I and II. f is the oscillator strength, m and e are the mass and the charge of the electron, V is the molar volume, and n is the number of the valence electrons per unit molecule.

The Grüneisen parameter for the electronic susceptibility as defined by $\chi'=-(d\ln\chi/d\ln V)$ is obtained as follows:

$$\chi'=1-\frac{\chi_{\text{I}}}{\chi}\frac{d\ln f_{\text{I}}}{d\ln V}-\frac{\chi_{\text{II}}}{\chi}\frac{d\ln f_{\text{II}}}{d\ln V}+\frac{2}{E_g}\left[\frac{E_g}{E_{\text{I}}}\frac{\chi_{\text{I}}}{\chi}\right]\frac{dE_{\text{I}}}{d\ln V}$$
$$+\frac{2}{E_g}\left[\frac{E_g}{E_{\text{II}}}\frac{\chi_{\text{II}}}{\chi}\right]\frac{dE_{\text{II}}}{d\ln V}\ . \tag{8}$$

For the chalcogenide amorphous semiconductors studied in the present paper the transition energy in region II is almost independent of pressure. We can then put $dE_{\text{II}}/d\ln V\approx 0$ and can neglect the fourth term in Eq. (8). The second and third terms together give $-(d\ln f/d\ln V)^*$, and this term is the change in oscillator strength.

As a result, Eq. (8) is simplified as follows:

$$\chi'\approx 1-\left[\frac{d\ln f}{d\ln V}\right]^*+\frac{2\eta}{E_g}\frac{dE_{\text{I}}}{d\ln V}\ , \tag{9}$$

where

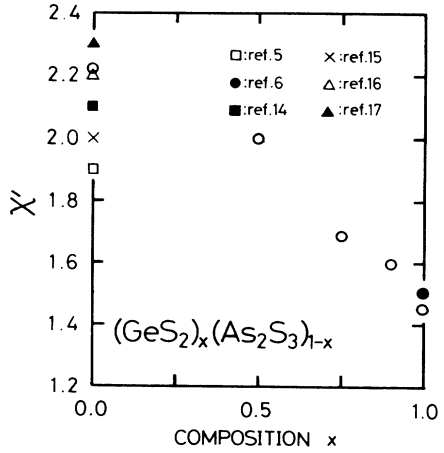

FIG. 12. The Grüneisen parameter for the electronic susceptibility by $\chi'=-d\ln\chi/d\ln V$ is plotted as a function of the composition x for $(GeS_2)_x(As_2S_3)_{1-x}$. The values of χ' from Refs. 5, 6, and 14–17 are also plotted.

$$\eta = E_g \chi_I / E_I \chi \ .$$

For the $(GeS_2)_x(As_2S_3)_{1-x}$ system, E_0 shifts to the red and $dE_I/d\ln V > 0$. If the change in oscillator strength is small, it follows that $\chi' > 1$.

χ' can be obtained from the experimentally obtained $(1/n)(dn/dP)$ by using the following relation:

$$\chi' = \frac{n^2}{n^2-1}\frac{2}{K}\left[\frac{1}{n}\frac{dn}{dP}\right] . \tag{10}$$

In Fig. 12, χ' obtained by this formula with the experimental data are plotted as a function of the GeS_2 composition x. For $x=1$, the value of $(1/nl)(dnl/dP) = 2.1\times10^{-3}$ kbar^{-1} from Ref. 6 is used. In the $(GeS_2)_x(As_2S_3)_{1-x}$ system, $\chi' \geq 1$ is seen to be true for every x, as in the case of other chalcogenide glasses, and χ' tends to decrease with increasing GeS_2 composition x. The values of χ' from Refs. 5, 6, and 14—17 are also shown in Fig. 12. These reported data are in good agreement with our experiment.

Further, the refractive index n is determined by all electronic transitions between the valence and conduction band, whereas the relatively weak optical absorption near the band-gap region is determined by a small number of transitions in the Urbach tail. When the interaction between the lone-pair electrons increases, the valence band broadens as described above. However, the mean density of states does not change and therefore the oscillator strength remains approximately constant. For this reason, the refractive index is not expected to show any anomalous change under pressure.

ACKNOWLEDGMENT

We would like to thank Professor Y. Toyozawa for his encouragement and discussion on the research of the optical absorption for a random system.

[1]A. Jayaraman, Rev. Mod. Phys. **55**, 65 (1983).
[2]J. A. Van Vechten, Phys. Rev. **182**, 891 (1969).
[3]M. Kastner, Phys. Rev. **6**, 2273 (1972).
[4]B. A. Weinstein, R. Zallen, and M. L. Slade, J. Non-Cryst. Solids **35&36**, 1255 (1980).
[5]B. A. Weinstein, R. Zallen, M. L. Slade, and A. deLozanne, Phys. Rev. B **24**, 4652 (1981).
[6]B. A. Weinstein, R. Zallen, M. L. Slade, and J. C. Mikkelsen, Jr., Phys. Rev. B **25**, 781 (1982).
[7]K. Murase, K. Yakushiji, and T. Fukunaga, J. Non-Cryst. Solids **43**, 37 (1981).
[8]J. M. Besson, J. Cernogora, and R. Zallen, Phys. Rev. B **22**, 3866 (1980).
[9]Ke. Tanaka, Phys. Rev. B **30**, 4549 (1984).
[10]J. C. Phillips, J. Non-Cryst. Solids **43**, 37 (1981).
[11]L. Ticha, L. Tichy, N. Rysava, and A. Triska, J. Non-Cryst. Solids **74**, 37 (1985).
[12]S. Abe and Y. Toyozawa, J. Phys. Soc. Jpn. **50**, 2185 (1981).
[13]Ke. Tanaka, Solid State Commun. **60**, 295 (1986).
[14]R. W. Dixon, J. Appl. Phys. **38**, 5149 (1967).
[15]A. Feldman, D. Horowitz, R. W. Waxlar, and M. J. Dodge, in Natl. Bur. Stand. (U.S.) Technical Note No. **993** (U.S. GPO, Washington, D.C., 1979), pp. 56—63.
[16]R. K. Galkiewicz and J. Tauc, Solid State Commun. **10**, 1261 (1971).
[17]R. M. Waxler, IEEE J. Quantum Electron. **QE-7**, 166 (1971).